Taylor & Francis
Taylor & Francis Group

Structural Engineering International

ISSN: (Print) (Online) Journal homepage: https://www.tandfonline.com/loi/tsei20

Estimation of the Structural Reliability for Fatigue of Welded Bridge Details Using Advanced Resistance Models

Davide Leonetti Asst. Prof. , H.H. (Bert) Snijder Prof. & Johan Maljaars Prof.

To cite this article: Davide Leonetti Asst. Prof. , H.H. (Bert) Snijder Prof. & Johan Maljaars Prof. (2020): Estimation of the Structural Reliability for Fatigue of Welded Bridge Details Using Advanced Resistance Models, Structural Engineering International, DOI: 10.1080/10168664.2020.1813675

To link to this article: https://doi.org/10.1080/10168664.2020.1813675

Published online: 20 Oct 2020.

Estimation of the Structural Reliability for Fatigue of Welded Bridge Details Using Advanced Resistance Models

Davide Leonetti, Asst. Prof.; **H.H. (Bert) Snijder**, Prof.; **Johan Maljaars**, Prof., Eindhoven University of Technology, Eindhoven, The Netherlands. Contact: d.leonetti@tue.nl

DOI: 10.1080/10168664.2020.1813675

Abstract

This present paper concerns the application of probabilistic fatigue life prediction models based on S–N curves aiming at the estimation of the safety level for a non-load carrying cruciform joint. The safety level is expressed in terms of the reliability index as a function of the number of applied cycles. Estimating the reliability of a structural component against fatigue failure is relevant for both new and existing structures. The analysis is executed considering three models. For each of them, the input random variables are given in a probabilistic manner, based on fatigue test data from the scientific literature. The effect of the model uncertainty on the model response is quantified for both the load and the resistance side, demonstrating its relevance. Moreover, it has been shown that a 0.5 to 1 increase in the reliability index is achievable by applying the newly proposed, more complex model.

Keywords: fatigue; steel bridges; welded joints; structural reliability; uncertainty

Introduction

The safety assessment of bridge structural details for fatigue failure, requires an appropriate resistance model representing the structural detail under consideration. Concerning bridge infrastructures, resistance models based on both S–N curves and fracture mechanics have been widely applied, either to show that the design life can be reached or to determine the safety status of such details. An S–N curve describes the empirical relationship between the applied stress range and the number of cycles to failure of a certain structural detail. The European standard EN 1993-1-9, Eurocode 3,[1] recommends a fatigue resistance model based on S–N curves characterizing the fatigue resistance under constant amplitude (*CA*) and variable amplitude (*VA*) loading. The characteristic *CA* S–N curve is derived from laboratory tests and presents the finite life region and the fatigue limit, i.e. the stress range value assumed as the threshold for fatigue failure under *CA* loading, see *Fig. 1*. For *VA* loading, the *CA* S–N curve is extended below the fatigue limit using a log-log linear relationship with a slope modified according to the findings of Haibach.[2] The Palmgren-Miner linear damage rule is used to consider the effect of *VA* loading, see *Fig. 1*. In Eurocode 3, partial factors are recommended to be applied that should be multiplied with to the characteristic values of strength to determine the design value based on the design type and consequences of failure. For a safe-life design two values of the partial factors, $\gamma_{M,f}$, are recommended: $\gamma_{M,f} = 1.35$ for high consequences of failure, $\gamma_{M,f} = 1.15$ for low consequences of failure.

The resistance model recommended in Eurocode 3 has been modified in,[3] mostly following the recommendations given in[4] to make it suitable for probabilistic analyses, aiming to determine the safety status expressed in terms of probability of failure P_f, or reliability index β. In particular, the variability of the fatigue resistance is modeled as a combination of the variability of the *CA* S–N curve and the critical damage, which are both recommended in the probabilistic model code of the JCSS.[4] Another option to estimate these quantities is to use a fatigue resistance model calibrated with test data, which need to be obtained using load histories similar to those faced during service.[5] This can be done by inferring fatigue test data using a probabilistic fatigue resistance model, as it was done in.[6,7]

Klippstein and Schilling[8] investigated the stress spectra resulting from the traffic loading of short-span bridges. The analyses indicated that the load history recorded can be reproduced by a stress spectrum following a truncated Rayleigh distribution. The same authors[9] performed fatigue tests under *CA* and *VA* loading, using the truncated Rayleigh stress spectrum, to characterize the response to fatigue loading of non-load carrying cruciform joints made of A572 Gr.50 steel. The fillet welds were produced by submerged arc welding, using Lincoln L61 wire and 761 flux. Also, Barsom[10] performed laboratory tests dedicated to the estimation of the fatigue crack growth rate under the truncated Rayleigh spectrum loading. These test data form the basis to calibrate fatigue resistance models in applications in which the loading spectrum can be assumed similar to a truncated Rayleigh. This is because they provide information about the non-linear phenomena of which a quantification is difficult in absence of test data.[5]

Two sources of uncertainty are to be considered in a fatigue reliability analysis. The aleatory uncertainty exists due to the intrinsic variability of the phenomenon under investigation in this case, the intrinsic variability of

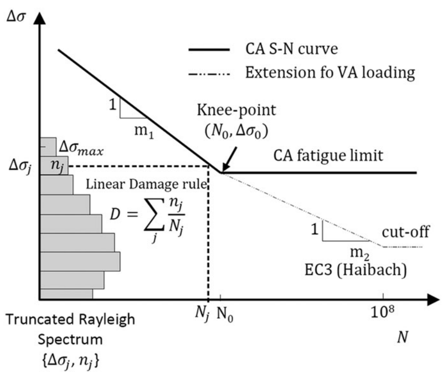

Fig. 1: Fatigue resistance model as defined in the Eurocode 3 (EN 1993-1-9)

the fatigue life. The epistemic uncertainty is related to the amount of information available to describe the phenomenon, in this case the amount of fatigue test data on which the S–N curve is based. For fatigue test data analysis these uncertainties have been quantified in,[6,7] amongst others.

The object of this study is to compare the predicted reliability according to the S–N curve in Eurocode 3 (EN 1993-1-9) with a more advanced model at the end of the design life. The model proposed in,[6] hereafter referred to as the modified six parameters random fatigue limit model (the modified 6PRFLM), is selected for the latter. These models are calibrated based on the test data produced by Klippstein and Schilling for a non-load carrying cruciform steel joint using the truncated Rayleigh spectrum.[8,9] Considering a characteristic fatigue resistance curve representing the detail under investigation, the applied stress spectrum is determined for an arbitrary design life equal to 10^7 cycles, and is assumed to follow a truncated Rayleigh distribution. In addition, the effect of the epistemic uncertainty on both load and resistance side is quantified to highlight their relevance with respect to the estimated safety status.

Models and Methods

In this work, the fatigue resistance under *VA* loading is estimated by making use of two different models based on S–N curves. The first model is the bilinear S–N curve, depicted in *Fig. 1*, applied in Eurocode 3 (EN 1993-1-9),[1] and the recommendation of the probabilistic model code from the JCSS.[4] The second model employed is the probabilistic fatigue life prediction model proposed in,[6] the modified 6PRFLM. Both models are briefly described in the two following sections.

The Bilinear S–N Curve

The bilinear S–N curve for fatigue resistance has been established after the findings of Haibach[2] and forms the basis of the deterministic fatigue life assessment of several standards and guidelines such as Eurocode 3 (EN 1993-1-9),[1] BS 7608,[11] and DNV-GL.[12] It is based on the Basquin relation for stress ranges higher than the fatigue limit, $\Delta\sigma_0$, and a log-log linear extension for considering the contribution to the fatigue damage of the stress ranges lower than the fatigue limit, see *Fig. 1*. The slope of the extension is assumed to be shallower than the slope of the Basquin relation. This is due to the fact that the stress ranges lower than $\Delta\sigma_0$ are less damaging than those above. This model makes use of the following form of the Basquin relation, which is a linear relationship between the base-10 logarithm of the fatigue life, N, and the base-10 logarithm of the stress range, $\Delta\sigma$:

$$\log_{10} N = a_1 + m_1 \log_{10} \Delta\sigma \quad \text{for } \Delta\sigma > \Delta\sigma_0 \tag{1}$$

the variable a_1 is the intercept of the curve for $\Delta\sigma = 1$, and m_1 is the slope. Stress ranges lower than the fatigue limit are accounted for by an exponential extrapolation of the S–N curve below the fatigue limit, of which the slope has been modified according to the findings of Haibach:

$$\log_{10} N = a_2 + m_2 \log_{10} \Delta\sigma \log_{10} \Delta\sigma \quad \text{for } \Delta\sigma \leq \Delta\sigma_0 \tag{2}$$

where m_2 is the slope and a_2 is the intercept of the curve. Variable a_1 is a random variable assumed to be fully correlated to a_2, which is also a random variable. Both are assumed to be lognormally distributed with mean value and standard deviation to be determined by inferring *CA* fatigue test data using the least square method. The value of a_2 is obtained considering that the fatigue limit is the stress range associated with a fatigue life equal to 5 million cycles.[1] In EN 1993-1-9, the extension is applied to the stress ranges lower than $\Delta\sigma_0$ and above the cut-off limit, defined as the stress range corresponding to 10^8 cycles, see *Fig. 1*. It results that the stress ranges lower than the cut-off limit are considered negligible. In the present work, the cut-off limit is neglected, following the JCSS Probabilistic Model Code.[4] The Palmgren-Miner linear damage rule is applied to determine failure under the effect of variable amplitude loading:

$$D = \sum \frac{n_j}{N_j} \tag{3}$$

where the index j refers to a stress range of the loading spectrum, n_j is the number of cycles associated with that stress range, and N_j is the number of cycles to failure predicted by the S–N curve. Failure occurs when the cumulated damage, D, reaches its critical value $D_{cr} = 1$ in EN 1993-1-9. In[4] the critical damage is assumed to be a lognormally distributed random variable having a mean value $\mu_D = 1$ and scale parameter $\sigma_D = 0.3$,[4] in order to consider the uncertainty associated with *VA* loading, which are due to load sequence effects.

The Modified 6PRFLM

This model for the inference of *VA* fatigue test data was proposed in[6,13] and its formulation is based on the 6PRFLM, developed for *CA* fatigue test data, but extended with the damage limit concept first proposed by Kunz[14] in combination with the linear damage rule of Palmgren and Miner.

The 6PRFLM makes use of the following relation between the base-10 logarithm of the fatigue life, N, and the base-10 logarithm of the stress range, $\Delta\sigma$:

$$\log_{10} N = \beta_0 + \beta_1 \log_{10} \Delta\sigma - p \log_{10}\left(1 - \frac{\Delta\sigma_0}{\Delta\sigma}\right) \tag{4}$$

where β_0 and β_1 are the model parameters that control the location and the slope of the curve in the finite life region, just as the variables a and m_1 do in the bilinear S–N curve, and p is the parameter controlling the curvature between the finite and the infinite life regions. The fatigue limit and the fatigue life conditional to the fatigue limit are modeled as random variables, namely V and $W|V$, respectively. V is modeled by the function f_V, which is a function of the base-10 logarithm of the fatigue limit $v = \log_{10}(\Delta\sigma_0)$ and is conditional to the location and scale parameters of the probability distribution associated with the fatigue limit, i.e. μ_V and σ_V:

$$f_V = \frac{1}{\sigma_V} \phi\left(\frac{v - \mu_V}{\sigma_V}\right) \tag{5}$$

where ϕ is the pdf of the standard normal distribution. In a similar way, $f_{W|V}$ is a function of the base-10 logarithm of the number of cycles to failure $w = \log_{10} N$ and is conditional to (1) the parameters β_0, β_1, p of the S–N curve, Eq. (4), (2) the applied stress range $\Delta\sigma$, and (3) the fatigue limit $\Delta\sigma_0$. These parameters determine the location parameter of W|V:

$$f_{W|V} = \frac{1}{\sigma_{W|V}} \phi \left(\frac{w - [\beta_0 + \beta_1 \log_{10}\Delta\sigma \quad - p\log_{10}(1 - (\Delta\sigma_0/\Delta\sigma))]}{\sigma_{W|V}} \right) \tag{6}$$

where $\sigma_{W|V}$ is the scale parameter of the distribution. Since the symbol ϕ denotes the standard normal distribution, the fatigue limit and the fatigue life conditional to the fatigue limit are both assumed to be lognormally distributed. The probability density and the cumulative distribution functions of w are:

$$f_W(w|\Delta\sigma,\ \theta_{CA}) = \int_{-\infty}^{\log_{10}\Delta\sigma} f_V\, f_{W|V}\, dv \tag{7}$$

$$F_W(w|\Delta\sigma,\ \theta_{CA}) = \int_{-\infty}^{\log_{10}\Delta\sigma} f_V\, F_{W|V}\, dv \tag{8}$$

where θ_{CA} is the vector of the 6PRFLM parameters, i.e. $\theta_{CA} = \{\beta_0,\ \beta_1,\ \sigma_{W|V},\ \mu_V,\ \sigma_V,\ p\}$ and $F_{W|V}$ is the cumulative distribution function of $W|V$.

The contribution of the different stress ranges to the fatigue damage D, is considered by using the linear damage rule, Eq. (3). To consider the stress ranges lower than the fatigue limit it is assumed that the threshold stress range for fatigue damage accumulation $\Delta\sigma_{th}$ is a function of the cumulated damage. In particular, it is assumed that:

$$\Delta\sigma_{th} = \Delta\sigma_0 \left(1 - \frac{D}{D_{cr}}\right)^{\zeta} \tag{9}$$

where D_{cr} is the critical value of the damage, and ζ is a model parameter controlling the trend of the normalized threshold stress range $\Delta\sigma_{th}/\Delta\sigma_0$ as a function of the normalized damage, or cycle ratio, D/D_{cr}.

D_{cr} has the same meaning as in the bilinear S–N curve, however, it is described by a distribution that is calibrated based on fatigue test data. D_{cr} It is assumed to be a lognormally distributed random variable having mean value μ_D and scale parameter σ_D. The vector of the model parameters is $\theta_{VA} = \{\mu_D,\ \sigma_D,\ \zeta\}$. θ_{CA} and θ_{VA} are estimated by respectively inferring CA and VA fatigue test data using the maximum likelihood method. Moreover, θ_{VA} is conditional upon θ_{CA}. This is because the 6PRFLM is first used to infer CA fatigue test data, determining θ_{CA} then, θ_{CA} is used in the 6PRFLM to infer VA fatigue test data and determine θ_{VA}.

Figure 2 shows the 6PRFLM and its horizontal and oblique asymptotes on a log-log scale in which the vertical axis is normalized to $\Delta\sigma_0$ and the horizontal axis is normalized to $N_0 = \beta_0 + \beta_1 \log_{10}(\Delta\sigma_0)$. The figure shows how the fatigue limit decreases with increasing the normalized damage assuming, for example, $\zeta = 1$, which implies that Eq. (9) is a linear relation between $\Delta\sigma_{th}$ and D/D_{cr}. Different from the bilinear model, a stress range $\Delta\sigma$ lower than $\Delta\sigma_0$ contributes to the fatigue damage only if the previously applied stress ranges induced a certain D/D_{cr} in such a way that the threshold stress range $\Delta\sigma_{th}$ is lower than this stress range $\Delta\sigma$. This is based on an analogy between the fatigue damage and the crack size, and is in agreement with fracture mechanics. Different from the modified 6PRFLM, in the bilinear model, all the stress ranges contribute to the fatigue damage since the first applied cycle, which is not in agreement with the mechanics of the fatigue phenomenon. This is because, the larger is the crack size, the larger is the damage, and the lower is the stress range which contributes to crack growth, i.e. damage accumulation. In *Fig. 2*, the modified 6PRFLM is plotted for $D/D_{cr} = 0.25$, 0.50, 0.75 and 1.

The 6PRFLM and the modified 6PRFLM are used to infer experimental data, CA and VA fatigue test data, respectively, using the maximum likelihood method, i.e. by maximizing the likelihood function, which is a function of the model parameters and is conditional to the data and the model:

$$L(\theta;\, Data) = \prod [f_w(w|\Delta\sigma,\ \theta)]^{\delta_i} [1 - F_w(w|\Delta\sigma,\ \theta)]^{1-\delta_i} \tag{10}$$

where δ is the failure indicator, i.e. $\delta = 1$ for failure in the finite life regime and $\delta = 0$ for runout in the infinite life regime. As a result of the maximization, the estimator of the model parameter is determined as well as the uncertainty. The epistemic uncertainty is modeled as a multivariate normal distribution of the model parameters, of which the mean value is the maximum likelihood estimator, and the covariance matrix is determined from the Fisher information matrix, which is the Hessian matrix of the Loglikelihood function, i.e. the matrix of the second derivatives, evaluated at the maximum likelihood estimator. More information can be found in.[6,13] In summary, the observed Fisher information matrix is used to estimate the epistemic uncertainty, and the aleatory uncertainty is modeled following the modified 6PRFLM. To evaluate the model response, i.e. the distribution of the fatigue life under VA loading, the Monte Carlo method is used. The epistemic and aleatory uncertainty are considered using a nested random sampling scheme. Therefore, for each simulation the value of θ_{CA} and θ_{VA} are sampled from the multivariate normal distribution of the model parameters, and consequently, the fatigue

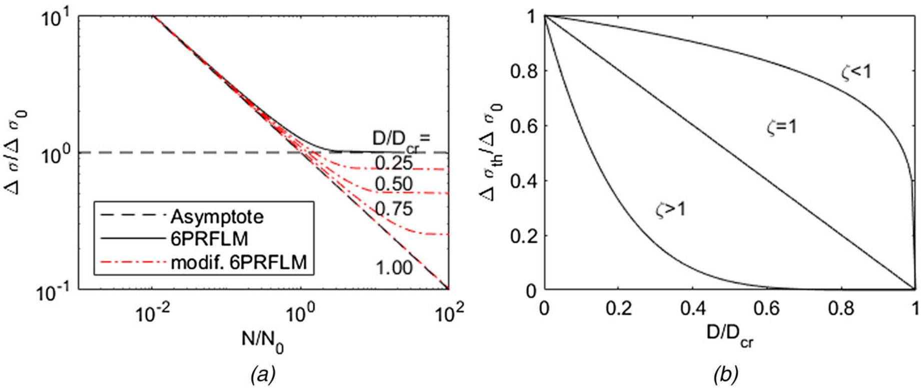

Fig. 2: (a) Modified 6PRFLM for D/D_cr = *0.25, 0.50, 0.75 and 1 and its asymptotes and (b) the damage limit function for different values of ζ*

life is estimated considering a random sample of the S–N curve, and the critical damage.

The Fatigue Resistance of the Non-Load Carrying Cruciform Joint

CA Fatigue Test Data

Several authors investigated the fatigue resistance of non-load carrying cruciform joints. The test data reported in the background documentation to EN 1993-19[15] are plotted in *Fig. 3a* and compared with the S–N curve given in EN 1993-1-9, the characteristic fatigue resistance for a fatigue life equal to 2 million cycles, i.e. the detail category. The welded detail under investigation is shown in *Fig. 3* and in EN 1993-1-9 is associated to the detail category 80. Moreover, *Fig. 3a* shows that the latter is a realistic lower bound curve for this population. *Fig. 3b* shows only the fatigue test data produced by Klippstein and Schilling[9] compared with detail category 80. It results that detail category 80 is significantly conservative with respect to these data. For this reason, a characteristic S–N curve has been derived using only the *CA* fatigue test data of,[9] see *Fig. 3b*, and the procedure used in EN 1993-1-9. This implies that the failed *CA* fatigue test data are inferred and the Basquin relation, Eq. (1), is fit to the failure data from[9] using the least square method, considering $x = \log_{10}(\Delta\sigma_{\max})$ as the independent variable, and $w = \log_{10}(N)$ is the dependent variable. The results are reported in *Table 1*.

The characteristic fatigue resistance curve is defined starting from the stress range corresponding to 2 million cycles for a probability of failure equal to 95% and 75% lower confidence bound, considering the standard deviation and the number of samples [Eurocode 3]. This requires the determination of a lower tolerance bound (*LTB*). At a certain stress range $\Delta\sigma$, the *LTB* is calculated by

$$\log_{10} N_{LTB} = \log_{10}\hat{N} + k_{P,1-\alpha}\,\hat{\sigma}_w \times \sqrt{1+\frac{1}{m_{CA}}+\frac{(\log_{10}\Delta\sigma - E[\log_{10}\Delta\sigma_j])^2}{\sum_j(\log_{10}\Delta\sigma_j - E[\log_{10}\Delta\sigma_j])^2}} \qquad (11)$$

where $\log_{10}\hat{N}$ is estimated using the Basquin relation, $k_{P,1-\alpha}$ is a coefficient for the calculation of the tolerance limit,[16] which is obtained from the non-central Student T distribution, and is a function of the selected percentile P, the confidence level α and the number of test data m_{CA}, $\hat{\sigma}_w$ is the estimator of the standard deviation of the residuals, reported in *Table 1*, the stress range $\Delta\sigma_j$ refers to the j-th test data, i.e. $j = 1 \ldots m_{CA}$, and $E[\cdot]$ is the expectation operator. The *LTB* curve for $P = 0.95$ and $\alpha = 0.75$ is plot in *Fig. 3b*. It results that the characteristic fatigue resistance for $N = 2$ million cycles is $\Delta\sigma_C = 126$ MPa, for the database of.[9] The characteristic S–N curve is constructed from this point, considering m_1 as obtained for the Basquin relation, *Table 1*. Its extension has been defined below the knee point located at 5 million cycles.[1] The

Parameter	a_1	m_1	σ_w
Estimator	14.9	−3.99	0.0733

Table 1: Estimators of the Basquin equation and its extension fitting the CA *failure data from Klippstein and Schilling*

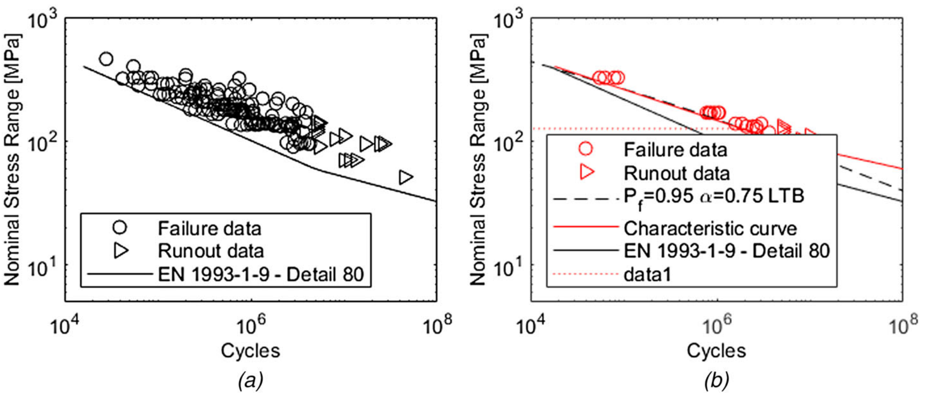

Fig. 3: CA *fatigue test data related to the non-load carrying cruciform joint: (a) all the data in the background document of EN1993-1-9, and (b) data from Klippstein and Schilling*

characteristic curve is also shown in *Fig. 3b*. It appears to be significantly higher than the S–N curve for detail category 80 recommended in the Eurocode 3 for the non-load carrying cruciform joint.

The 6PRFLM, Eq. (4) has been used to infer the same dataset. The estimators of the parameters are reported in *Table 2*. It can be seen that the estimators of β_0, β_1 and $\sigma_{w|v}$ are the same as a_1, m_1 and σ_w obtained for the Basquin relation. This results in the two models to be very close in the finite life region. On the contrary, the 6PRFLM allows the estimation of the fatigue limit $\Delta\sigma_0 = 10^{\mu_v}$, and its scatter σ_v, based on the distribution of failure data and runouts, which is not possible using the Basquin relation. In addition, the parameter p allows modeling the curvature between finite and infinite life regions, see *Fig. 2*. However, p being almost equal to 0 means that in this case a sharp knee is obtained for the median S–N curve. This is attributed to the small number of data around the knee-point.

The Rayleigh Stress Spectrum and *VA* Fatigue Test Data

This section presents the *VA* fatigue test data and describes the loading spectrum used in this investigation. The normalized stress spectrum follows a truncated Rayleigh distribution as a result of the findings in[8] regarding the loading spectrum in short span bridges. The truncated Rayleigh distribution is given by the following relationship:

$$f(z) = C_R\, z \exp(-0.5\, z^2) \quad \text{for } 0 < z \le z_{\max} \qquad (12)$$

where z is the normalized stress range, $f(z)$ is the normalized frequency, $z_{\max}$ is the truncation level, and C_R is a normalizing constant due to the truncation, being $C_R = 1/(0.988)$ for $z_{\max} = 3$. The normalized spectrum is shown in *Fig. 4a*. The stress range is

$$\Delta\sigma = \Delta\sigma_{\min} + z\,\Delta\sigma_d \qquad (13)$$

where $\Delta\sigma_d = (\Delta\sigma_{\max} - \Delta\sigma_{\min})/z_{\max}$ is the dispersion stress range, $\Delta\sigma_{\min}$ is the minimum stress range in the spectrum, see *Fig. 4a*. In[9] the stress spectra were generated considering $\Delta\sigma_d = \Delta\sigma_m$. Then, for $z_{\max} = 3$ the

Parameter	Estimator	St.err	Correlation Matrix					
			β_0	β_1	$\sigma_{w\|v}$	μ_v	σ_v	p
β_0	14.9	0.387	1	−0.995	0.341	0.205	−0.313	−0.621
β_1	−3.99	0.159	−0.995	1	−0.283	−0.175	0.258	0.554
$\sigma_{w\|v}$	0.0733	0.0208	0.341	−0.283	1	0.471	−0.687	−0.602
μ_v	2.11	0.0122	0.205	−0.175	0.470	1	−0.630	−0.408
σ_v	0.0383	0.0279	−0.313	0.258	−0.688	−0.630	1	0.701
p	$1.09\ 10^{-8}$	0.0709	−0.621	0.554	−0.602	−0.408	0.701	1

Table 2: Estimators and uncertainty of the 6PRFLM fitting the CA *data from Klippstein and Schilling*

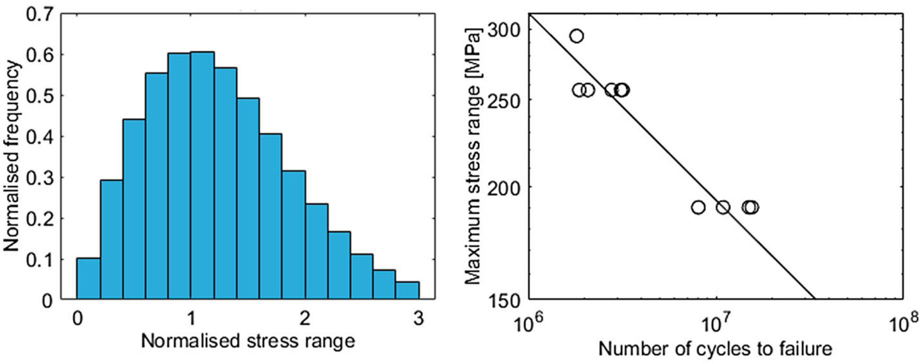

(a) (b)

Fig. 4: (a) Normalized Rayleigh spectrum and (b) VA *fatigue test data from [9] fitted by the* LRM

maximum stress range of the spectrum is $\Delta\sigma_{\max} = \Delta\sigma_{\min} + 3\,\Delta\sigma_d$, and the modal, i.e. the most frequent, stress range in the spectrum is $\Delta\sigma_m = \Delta\sigma_{\min} + \Delta\sigma_d$. Therefore, given the truncation level, and given that the fatigue test data used for calibrating the modified 6PRFLM are produced using $\Delta\sigma_{\min} = 0$, only one parameter among $\Delta\sigma_m$, $\Delta\sigma_d$, and $\Delta\sigma_{\max}$ is necessary to fully define the shape of the stress spectrum. In this work, $\Delta\sigma_{\max}$ is used, which is based on the approach proposed by Gassner while defining the Gassner curve. Different authors inferred *VA* fatigue test data obtained with the same type of stress spectrum using different stress range values to identify the stress spectrum.[17]

The *VA* fatigue test data produced in[9] using the Rayleigh stress spectrum described by Eqs. (12) and (13) are depicted in *Fig. 4b* by plotting on a log-log scale the maximum applied stress range of the spectrum against the number of cycles to failure. The *VA* fatigue data refer to specimens belonging to the same batch of the specimens used for the *CA* fatigue tests described in the previous section. Moreover, the geometry and production procedure are also the same. The *VA* fatigue test data are inferred using a linear regression model (*LRM*):

$$w = \alpha_0 - \alpha_1 x + \epsilon(0, \sigma_w) \qquad (14)$$

where $w = \log_{10}(N)$ is the dependent variable, $x = \log_{10}(\Delta\sigma_{\max})$ is the independent one, α_0 and α_1 are the model parameters, and ϵ is the error term for which it is assumed that the residuals follow a normal distribution having zero mean and standard deviation equal to σ_w. The estimators of the model parameters are reported in *Table 3*. This model allows a comparison between the prediction of the modified 6PRFLM and the bilinear S–N curve of EN 1993-1-9 with test data in a probabilistic fashion.

Parameter	α_0	α_1	σ_w
Estimator	18.0	−4.81	0.113

Table 3: Estimators of the parameters of the LRM *fitting the* VA *fatigue test data*

The bilinear model has not been used to infer the *VA* fatigue test data, since the value of m_2 is obtained from the slope of the Basquin relation using the Haibach rule: $m_2 = m_1 - 2$, and a_2 is fully correlated to a_1. Moreover the critical damage is assumed to be lognormal random variable with mean $\mu_D = 1$ and scale parameter $\sigma_D = 0.3$, as reported in the JCSS Probabilistic Model code.[4] The Likelihood, the Akaike and the Bayesian Information Criteria resulting from the application of these models inferring the considered data were calculated in,[6] showing that the modified 6PRFLM confers higher likelihood to the considered data, and that the AIC and BIC statistics are in favor of the modified 6PRFLM.

The *VA* fatigue test data have been inferred also using the modified 6PRFLM, allowing the estimation of θ_{VA} and the epistemic uncertainty, which is given in *Table 4*. The random variable describing the epistemic uncertainty follows from the application of the Maximum Likelihood method and is assumed to be a multivariate Normal distribution of the model parameters as in.[6,7] It results that the critical damage distribution has a mean value 1.61 times higher and a lower scatter than assumed by the JCSS Probabilistic Model code.

Results

This section aims to compare the reliability index predicted by the different models at the end of the design life for the non-load carrying cruciform joint of which the *CA* and *VA* test fatigue test data have been presented and used to calibrate the models. At first, the reliability indices are compared considering the aleatory uncertainty only. In a second step, the epistemic uncertainty on the resistance side is added, and in the last step, the epistemic uncertainty is introduced for both the resistance and the load.

The calculation is performed by using the Monte Carlo Method. The general definition of the reliability index is used:

$$\beta = -\Phi^{-1}(P_f) \qquad (16)$$

where Φ^{-1} is the inverse of the cumulative standard normal distribution and P_f is the probability of failure, i.e. the ratio between the number of

Parameter	Estimator	St.err.	Correlation matrix		
μ_D	**1.61**	**0.161**	μ_D	σ_D	ζ
σ_D	0.225	0.0982	0.249	1	0.550
ζ	1.14	1.07	0.0243	0.550	1

Table 4: Estimators of the parameters of the modified 6PRFLM

simulations that showed failure before the end of design life ($D = 1$ at 10^7 cycles) and the total number of simulations.

The Rayleigh stress spectrum applied in this work has been calibrated to obtain a design life of 10^7 cycles, i.e. $D = 1$ at 10^7 cycles, and considering the design S–N curve, which results from the characteristic S–N curve by applying a partial factor $\gamma_{M,f}$. The characteristic S–N curve has been derived using the *CA* data from.[9] Calibrating the stress spectrum implies, since $\Delta\sigma_{\min} = 0$, $z_{\max} = 3$, and $\Delta\sigma_d = \Delta\sigma_m$, calibrating solely $\Delta\sigma_{\max}$. By using the characteristic S–N curve defined in the previous section, the Rayleigh stress spectra for a design life equal to 10^7 cycles are determined for safe life design considering the partial factors given in EN 1993-1-9 for both high and low consequences of failure. The maximum stress ranges of the stress spectrum are $\Delta\sigma_{\max} = 140$ and 119 MPa for $\eta_{M,f} = 1.15$ and 1.35, respectively.

The trend of the reliability index is depicted in *Fig. 5* as a function of the number of cycles resulting from both models including and excluding the epistemic uncertainty on the resistance side. It has been obtained by 10^7 Monte Carlo samples of the fatigue life. By doing so, assuming as a rule of thumb that a negligible numerical error is obtained with 100 failures, i.e. $P_f = 100/10^7$, a realistic estimation of the reliability is obtained for $\beta < 4.26$. When only aleatory uncertainty are considered, the modified 6PRFLM and the bilinear S–N curve show a similar scatter. Instead, when epistemic uncertainty are considered, the modified 6PRFLM results in a wider distribution than the bilinear S–N curve of EN 1993-1-9. This is because a steeper trend denotes a narrower, i.e. less scattered, distribution of fatigue life. This directly follows from Eq. (15). *Fig. 5a* shows the probability density function (Pdf) of two assumed distributions of the fatigue life, having their mean equal to 106 cycles and their CoV equal to 0.2 and 0.3, respectively. The cumulative density function (Cdf) is plotted for the same cases in the same figure. The reliability index is calculated using Eq. (15) and is plot in *Fig. 5b*. These figures show that the more scattered distribution results in a shallower trend of the reliability index.

Moreover, the results obtained using the modified 6PRFLM are closer to those obtained by the application of the *LRM* fitting the *VA* fatigue test data. It appears that the effect of the epistemic uncertainty is larger for the modified 6PRFLM than for the bilinear S–N curve of EN 1993-1-9. This shows in two differences. (1) For the bilinear S–N curve, the uncertainty related to the S–N curve extension and that related to the location of the fatigue limit is assumed to be fully correlated to the epistemic uncertainty associated with the location parameter of the *CA* S–N curve. In the modified 6PRFLM, the fatigue limit is modeled as a random variable of which the location and scale parameters result to be weakly correlated with the location parameter of the *CA* S–N curve, see *Table 2*. (2) In the modified 6PRFLM, the stress ranges below the fatigue limit are taken into account by the damage limit model, which is dependent on the value of ζ, assumed to be uncorrelated to any of the parameters of the *CA* S–N curve, since *CA* and *VA* data are inferred in two separate procedures. In summary, it appears that the epistemic uncertainty is not properly accounted for in the probabilistic fatigue resistance model constructed based on clause 9.6.1(5) of EN 1993-1-9, since it is only estimated on the basis of *CA* fatigue test data. For the considered design life, i.e. 10^7, and low consequences of failure, and when both the aleatory and the epistemic uncertainties are considered, the prediction of the bilinear S–N curve of EN 1993-1-9 is the most conservative, followed by the *LRM* and the modified 6PRFLM, see *Fig. 5a*. The difference between the prediction of the *LRM* of the *VA* fatigue test data and the modified 6PRFLM is due to the values of $\Delta\sigma_{\max}$ considered being outside the range of the *VA* fatigue test data used to calibrate the models. This makes the *LRM* the most conservative. For the *LRM*, the effect of the uncertainty increases with increasing the difference between $\Delta\sigma_{\max}$ and the stress range of the centroid of the data, i.e. $E[\log_{10}\Delta\sigma_j]$, see Eq. (11). This also explains the large difference between the *LRM* with and without the epistemic uncertainty. Moreover, the *LRM* does not include any type of threshold condition for fatigue failure under *VA* loading. This explains the fact that the difference between the modified 6PRFLM and the *LRM* increases with decreasing $\Delta\sigma_{\max}$. *Figure 6* also shows that the *LRM* gives very large effect of the epistemic uncertainty, as compared to the other two models. This is due to the low number of data (10 data) inferred by this model, as only *VA* fatigue test data were used. On the contrary, the bilinear S–N curve gives the smallest effect of the epistemic uncertainty due fact that only the *CA* test data (20 failure data and 9 runouts) were inferred by this

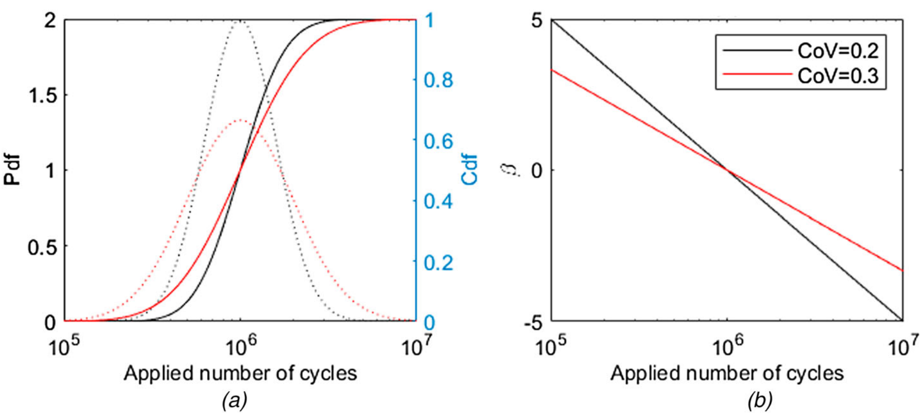

Fig. 5: Relation between the reliability index and the scatter of the fatigue life: (a) Pdf and Cdf of the fatigue life, and (b) trend of the reliability index

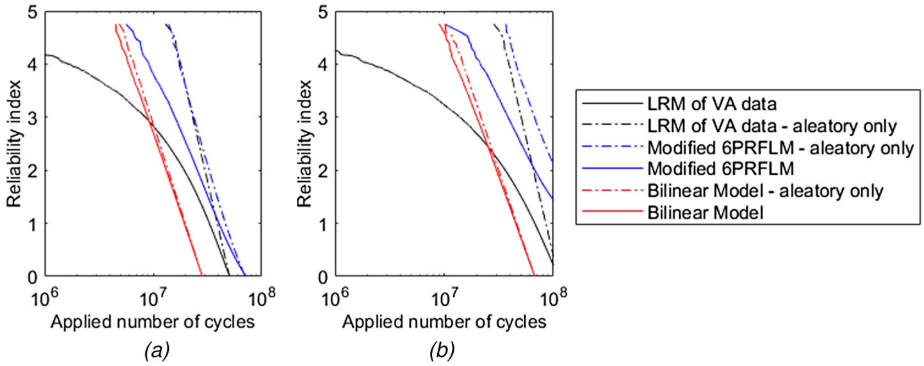

Fig. 6: Reliability index as a function of the applied number of cycles for the stress spectra resulting in a design life of 10^7 cycles: (a) low consequences of failure ($\Delta\sigma_{\max} = 140$ MPa), (b) high consequences of failure ($\Delta\sigma_{\max} = 119$ MPa)

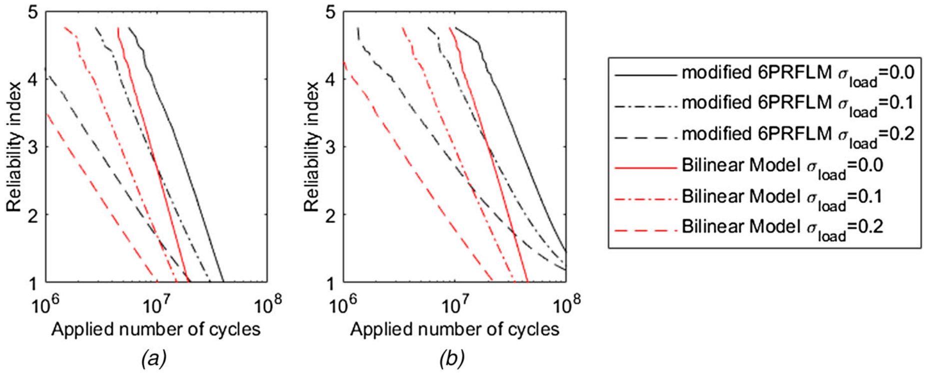

Fig. 7: Effect of load uncertainty on model response on the reliability index versus applied number of cycles for the stress spectra resulting in a design life of 10^7 cycles: (a) low consequences of failure($\Delta\sigma_{\max} = 140$ MPa), (b) high consequences of failure ($\Delta\sigma_{\max} = 119$ MPa)

model. The modified 6PRFLM incorporates both *CA* and *VA* data and highlights two aspects. On one hand, it shows the importance of corroborating *VA* fatigue test data with *CA* fatigue test data in order to reduce uncertainty. On the other hand, it shows the large epistemic uncertainty associated with *VA* loading.

The uncertainty on the load side has been modeled as a global model uncertainty, as suggested in the JCSS.[4] In here, the stress ranges of the truncated Rayleigh spectrum are multiplied by a lognormally distributed random variable with a mean of 1, and assuming full correlation between the stress range levels. Three values for the standard deviation on the load side, σ_{load} have been considered: 0, 0.1, and 0.2. The JCSS recommends $\sigma_{load} = 0.1$. *Figure 7* depicts the reliability index with and without the uncertainty associated with the load determination. In this case, the epistemic uncertainty associated with the resistance model is always considered. The Monte Carlo samples are generated performing a (independent) nested sampling of epistemic and aleatory uncertainty for both the load and resistance side. The figure shows that with increasing the uncertainty on the load side, i.e. stepwise increasing σ_{load} by 0.1, the reliability index at the end of the design life almost decreases by a unit value. This suggests a large importance of correctly estimating the uncertainty on the load side.

Conclusions

In this work, three fatigue resistance models were applied to estimate the reliability against fatigue failure of a non-load carrying cruciform joint and the effect of the uncertainty on both load and resistance sides. The following conclusions can be drawn:

(1) The bilinear S–N curve based on the linear regression of *CA* fatigue test data, the Haibach rule, and the recommendations from JCSS, which forms the basis of the S–N curves in EN 1993-1-9, is solely based on *CA* fatigue test data. This determines that the prediction of the reliability index differs from the modified 6PRFLM and the *LRM* of *VA* data when only aleatory uncertainty are considered. Moreover, the effect of the epistemic uncertainty is significantly smaller compared to the other two models, given the datasets inferred.

(2) The linear regression of *VA* fatigue test data determines a prediction in line with the modified 6PRFLM when the epistemic uncertainty on the resistance side is neglected. When epistemic uncertainty is taken into account, the linear regression model becomes significantly more conservative than the modified 6PRFLM. The conservativism increases with the maximum stress range of the spectrum $\Delta\sigma_{\max}$ approaching the fatigue limit $\Delta\sigma_0$ and with increasing the absolute value of the difference between the maximum stress range $\Delta\sigma_{\max}$ and the stress range at the centroid of the data. This proves the importance of corroborating *VA* fatigue test data with *CA* fatigue test data in a model for *VA* fatigue life prediction.

(3) The modified 6PRFLM is used to infer both *CA* and *VA* fatigue test data and is considered more reliable with respect to the other two models because it is able to take into account both *CA* and *VA* fatigue test data.

(4) Introducing the uncertainty on the load side has a significant effect on the estimated reliability index. In this case, a stepwise increase of σ_{load} associated to the load side by 0.1 resulted in approximately a unit decrease of the reliability index for all the considered models fitting the *CA* and *VA* data reported by Klippstein and Schilling.[9]

(5) For the considered datasets, it has been shown that increasing the model complexity leads to higher accuracy of the prediction and reduced uncertainty. Due to the model complexity and increasing calculation time, it is expected that such models are of better use for reliability analyses and for calibrating partial factors rather than for daily use in practice as their use requires also the application of statistical concepts.

Acknowledgements

The authors would like to thank the Dutch infrastructural asset owners ProRail and Rijkwaterstaat and the international organization TNO for their support.

ORCID

Davide Leonetti http://orcid.org/0000-0002-7436-3977
H.H. (Bert) Snijder http://orcid.org/0000-0002-2127-9886
Johan Maljaars http://orcid.org/0000-0001-5831-2478

References

[1] CEN, European Committee for Standardization. *EN1993-1-9: Eurocode 3: Design of Steel Structures, Part 1-9: Fatigue.* European Standard: Brussels, 2005.

[2] Haibach E. The allowable stresses under variable amplitude loading. In *Proceeding Conf. Fatigue Welded Struct.*, Gurney TR (ed), TWI – The Welding Institute: Cambridge, 1970, 328–339.

[3] Leander J. Reliability evaluation of the Eurocode model for fatigue assessment of steel bridges. *J. Constr. Steel Res.* 2018; **141**: 1–8.

[4] JCSS, probabilistic model code – part 3. *Jt. Comm. Struct. Saf.* 2000.

[5] Sonsino C. Principles of variable amplitude fatigue design and testing. *J. ASTM Int*. 2004; **1**: 19018.

[6] Leonetti D, Maljaars J, Snijder HH. Probabilistic fatigue resistance model for steel welded details under variable amplitude loading – inference and uncertainty estimation. *Int. J. Fatigue*. 2020; **135**: 105515.

[7] D'Angelo L, Nussbaumer A. Estimation of fatigue S–N curves of welded joints using advanced probabilistic approach. under review: IJFATIGUE-D-16-00685. *Int J Fatigue*. 2017; **97**: 98–113.

[8] Klippstein K, Schilling C. Stress spectrums for short-span steel bridges. In *Fatigue Crack Growth under Spectr. Loads.*, Wei R and Stephens R (eds), ASTM International: West Conshohocken, PA, 2009: 203–216.

[9] Klippstein KH, Schilling CG. Pilot study on the constant and variable amplitude behavior of transverse stiffener welds. *J. Constr. Steel Res.* 1989; **12**: 229–252.

[10] Barsom J. Fatigue crack growth under variable-amplitude loading in various bridge steels. In *Fatigue Crack Growth under Spectr. Loads.*, Wei R and Stephens R (eds), ASTM International: West Conshohocken, PA, 1976: 217–232.

[11] BS 7608. Guide to fatigue design and assessment of steel products. *Br. Stand.* 2014.

[12] DNV-GL, DNVGL-RP-C203. Fatigue Design of Offshore Steel Structures. *Recomm. Pract.* 2016.

[13] Leonetti D, Maljaars J, Snijder HH. Fitting fatigue test data with a novel S–N curve using frequentist and Bayesian inference. *Int. J. Fatigue.* 2017; **105**: 128–143.

[14] Kunz PM, Kulak GL. Fatigue safety of existing steel bridge. In Extending Lifesp. *Struct. San Fr. IABSE Symp*. 1995.

[15] Sedlacek G, Hobbacher A, Schleich JB, Nussbaumer A, Maddox SJ, Brozzetti J. First draft of the background document prEN 1993-1-9, 2003.

[16] Euler M, Kuhlmann U. *Statistical Intervals for Evaluation of Test Data According to Eurocode 3 Part 1–9*. University of Stuttgart, 2013.

[17] Fisher JW, Mertz DR, Zhong A. Steel bridge members under variable amplitude long-life fatigue loading. *Natl. Coop. Highw. Res. Progr. Rep*. 1983. https://trid.trb.org/view/201807